FINAL REPORT
U.S. Department of Energy

DEVELOPMENT OF MONITORING AND DIAGNOSTIC METHODS FOR ROBOTS USED IN REMEDIATION OF WASTE SITES

Principal Investigator: Michael Martin
Institution: Foster-Miller Technologies, Inc.
Collaborators: Dr. Joseph Cavallaro and Martin Leuschen
Institution: Rice University
Collaborator: Dr. Ian Walker
Institution: Clemson University

Project Number: 60040
Grant Number: DE-FG07-97ER14830
Grant Project Officers: Dr. Robert E. Price and Chester E. Miller
Project Duration: 09/15/97 to 03/14/00

TABLE OF CONTENTS

LIST OF FIGURES 3

EXECUTIVE SUMMARY 4

1.0 RESEARCH OBJECTIVES 5

2.0 METHODS AND RESULTS 6
- 2.1 Component Selection and Test Rig Design 6
- 2.2 Fault Selection and Simulation Methods 8
- 2.3 Instrumentation and Data Acquisition 12
- 2.4 Fault Insertion Procedure 14
- 2.5 Analytical Techniques 15
  - 2.5.1 Analytical Redundancy 15
  - 2.5.2 Derived Variables, Statistical and Spectral Analysis 16
- 2.6 Test Results 16
  - 2.6.1 Wheel Motor Fault Testing 17
  - 2.6.2 HPSS Fault Testing 19
  - 2.6.3 Advanced Fault Testing 24
- 2.7 Conclusions and Recommendations 24

3.0 RELEVANCE, IMPACT AND TECHNOLOGY TRANSFER 25
- 3.1 Research Focus on Critical DOE Problems 25
- 3.2 Research Contribution to Improved Technologies and Cleanup Approaches 25
- 3.3 Research Contribution to Bridge Gap between Fundament Research and Applied Technology 25
- 3.4 Project Impact 25
- 3.5 Justification for Larger-Scale Trials 25
- 3.6 Improved Scientific Capabilities 26
- 3.7 Advances in Understanding of Technology 26
- 3.8 Additional Scientific Hurdles 26
- 3.9 Interest Expressed by Other Parties 26

4.0 PROJECT PRODUCTIVITY 27

5.0 PERSONNEL SUPPORTED 27

6.0 PUBLICATIONS 27

7.0 INTERACTIONS 28

8.0 TRANSITIONS 28

9.0 PATENTS 28

10.0 FUTURE WORK 28

REFERENCES 29

1.0 LIST OF FIGURES

Figure 1. Test Rig Layout 7
Figure 2. Test Rig Hydraulic Schematic 7
Figure 3. Test Rig Assembly 8
Figure 4. Test Rig Control and Data Acquisition System 13
Figure 5. Data Acquisition System and Control Station 13
Figure 6. Data Acquisition Control Panel 14
Figure 7. Fault 9: Open Control Valve Winding 18
Figure 8. Fault 10: Sticking Control Valve 18
Figure 9. Fault 12: Loss of Resolver Feedback 20
Figure 10. Fault 13: Internal Leak in Drive Motor 20
Figure 11. Fault 1: Hydraulic Efficiency Change 21
Figure 12. Fault 3: Pump Drive Motor Fault 22
Figure 13. Fault 4: Loss of Cooling Oil 23
Figure 14. Fault 5: Scored Pump Housing 23
Figure 15. Fault 7: Broken Relief Valve Spring 24

EXECUTIVE SUMMARY

In the Environmental Management Science Program (EMSP) of the Department of Energy (DOE), extensive use of robots is planned for safe and efficient cleanup of hazardous and radioactive waste sites. Robots operating at these waste sites will be exposed to a variety of life-limiting environmental and operational conditions. Undetected faults can have serious consequences, and development of effective Monitoring and Diagnostic (M&D) methods will provide for early-stage detection, isolation, and tracking of developing faults before serious failures occur. More efficient M&D methods support the mission of DOE to provide safe, reliable, less costly cleanup of hazardous waste sites.

This research project focused on hydraulically driven robots of the type used in waste site remediation. Implanted fault tests were performed on a robot hydraulic drive to extract failure indications from the test data and develop meaningful, reliable diagnostic techniques. A test rig was designed and built, a list of fault implantation methods devised, and a successful test program conducted. A new theoretical fault-detection technique was developed, and project results indicate its effectiveness to detect faults.

This research was a collaborative effort involving Foster-Miller Technologies (FMT), Rice University, and Clemson University. Rig design and the test program were performed at FMT, with the universities supporting development and application of fault detection techniques and data analysis.

This project is the first evaluation of model-based diagnostics to hydraulic robot systems. A greater understanding of fault detection for hydraulic robots has been gained, and a new theoretical fault detection model developed and evaluated. The relevance to the EMSP is that these methods are effective for application to fault detection in hydraulic robot systems. Better fault detection for robots that must operate in hazardous environments will reduce the costs associated with their failures. Application of these methods will increase confidence in the safety of robot systems and thus lead to their increased use. The timeliness and effectiveness of DOE cleanup operations will ultimately benefit from this technology.

1.0 RESEARCH OBJECTIVES

In the Environmental Management Science Program of the Department of Energy (DOE), extensive use of robots is planned for safe and efficient cleanup of hazardous and radioactive waste sites. Robots operating at these waste sites will be exposed to a variety of life-limiting environmental and operational conditions. Undetected faults in these robots can have serious consequences, which include damage to the waste containment facilities by the faulty robot, complete or partial robot failure, or loss of the robot. Development of effective Monitoring and Diagnostic (M&D) methods will provide for early-stage detection, isolation, and tracking of developing faults before they result in serious failure. More efficient M&D methods would help DOE personnel reduce the risk of catastrophic in-site robot failures, decreasing the risk of containment facility damage, loss of robot and mission failures, and thus supporting faster, safer, and less expensive cleanup by avoiding the additional time and cost associated with robot failures.

To perform robot M&D, there are several methods proven to provide early detection of incipient faults. However, all of these methods are limited in application to electrically driven robots. The utility and effectiveness of these methods in application to remediation robots, which are typically hydraulic in nature, have never been proven. The research conducted in this project targeted the development of efficient M&D methods for hydraulic robots and was based on an extensive analysis of the M&D needs of remediation robots conducted under DOE Contract DE-AR-21-95MC32093 (Jammu, 1997).

In the work performed by Jammu (1997), the Rosie Mobile Worksystem was selected as a reference and divided into four subsystems: hydraulic power supply (HPSS); wheel motor, steering, and extension; heavy manipulator; and tether drive. Individual components in these subsystems were listed and their possible failure modes compiled. Each failure mode was assigned representative criticality, probability, and speed-of-failure values. A fault tree analysis was performed for each subsystem to identify the origin and propagation of failures. Criticality categories of levels were assigned to each component. The results of this extensive analysis indicated that faults in the HPSS and the tether drive had the most critical need for M&D.

To build on this work, the focus of the subject research was to perform implanted fault tests on a hydraulic subsystem of Rosie, specifically the HPSS and the wheel motor, in order to extract failure indications from test data and develop meaningful and reliable diagnostic techniques. The specific research objectives were to:

1. Assemble a test rig to serve as a model of a hydraulic component loop and provide a means to subject the test rig to realistic loads to simulate operation in service. The test rig must be instrumented to allow acquisition and monitoring of key parameters by a data acquisition system.
2. Develop a list of faults for implantation in the test rig.
3. Insert the predetermined faults into the test rig and record and analyze the resulting behavior using several types of analytical techniques to determine their effectiveness in providing early fault indication. Analytical redundancy (AR), an innovative model-based diagnostic technique, and traditional techniques such as derived variables, statistical, and spectral analysis will be used.
4. Develop data reduction technology to diagnose these faults in an early stage of development.

As described in Section 2, the research demonstrated the effectiveness of the AR method to detect faults in hydraulic subsystems and provides a basis for extension of this model-based technique to detect a full range of faults in a complete robot system. The diagnostic innovation represented by this model will further the progress needed to ensure effective M&D of robot systems used in DOE cleanup operations.

2.0 METHODS AND RESULTS

This section details the methods used and results obtained during the research performed to develop M&D methods for hydraulically actuated robots.

2.1 Component Selection and Test Rig Design

The goal of this project was to perform implanted fault tests on components of hydraulically actuated robots in order to extract failure indications from the test data and develop meaningful and reliable diagnostic techniques. Although it was not practical to perform these tests on an actual robot, simple, subscale tests ran the risk of producing results that were not meaningful or would not "scale up" to full-size components. With this in mind, the following guidelines were established to guide component selection and test rig design:

- Isolate specific subsystems and/or component types representative of those in hydraulically actuated robots. From these, select a limited number of individual components that can show a variety of failure modes and have relatively high criticality.
- Select individual components that are the same as, or closely represent, those used in Rosie and hydraulically driven robots of a similar scale.
- Power and control these components with a representative HPSS and servo control valves.
- Subject the components to realistic loads during test.
- Measure enough parameters during testing to maximize the chances of obtaining valid failure signatures.

Of the many potential components in Rosie, the hydraulic wheel motor, rotary actuator, and linear actuator best met the above guidelines. Any of these would need to be controlled, subjected to loading of some kind, and powered by a hydraulic power supply. These components were further evaluated based on the highest potential payoff to the project, their applicability to a range of robots, simulation of "nontrivial" failure modes, and affordability to the project.

Following the evaluation, the hydraulic wheel motor was selected as the test component, and one identical to the Rosie motor was used in the test rig. This Black Bruin Model 404-080-2111 from Valmet Power Transmission Inc. is a radial piston design with a maximum power rating of 35 kW (47 hp). The motor has a maximum output speed of 185 rpm and can deliver a torque of 2990 N-m at 250 bar (2205 ft-lb @ 3600 psi). Since it can drive a wheel directly and accept a substantial radial load, the exact value of the load depends on the axial location of the load with respect to the motor.

This hydraulic wheel motor was combined with several other components to form the test rig (see Figures 1, 2, and 3). The wheel motor was powered by a control valve in a velocity control loop and a commercial hydraulic power supply (20 gpm at 3000 psi). Both were similar to that used in Rosie.

The output shaft was loaded radially by means of an adapter and a hydraulic jack assembly. The radial load simulated the dead weight of the robot on a single wheel. For Rosie, this load is approximately 4000 lb. Additional load (simulating climbing, etc.) was applied to the wheel motor by an identical hydraulic motor operated as a pump. The pump motor connected to the wheel motor through a flexible coupling. The pump motor was fed through a separate hydraulic supply consisting of a low-pressure pump, cooler, and reservoir. A variable throttling valve was used to load the wheel motor, restricting the output of the pump.

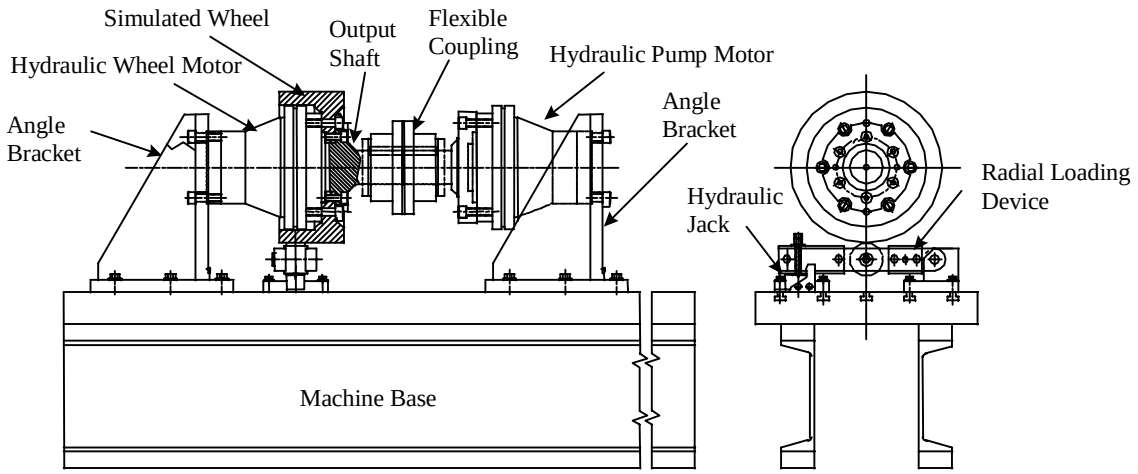

Figure 1. Test Rig Layout

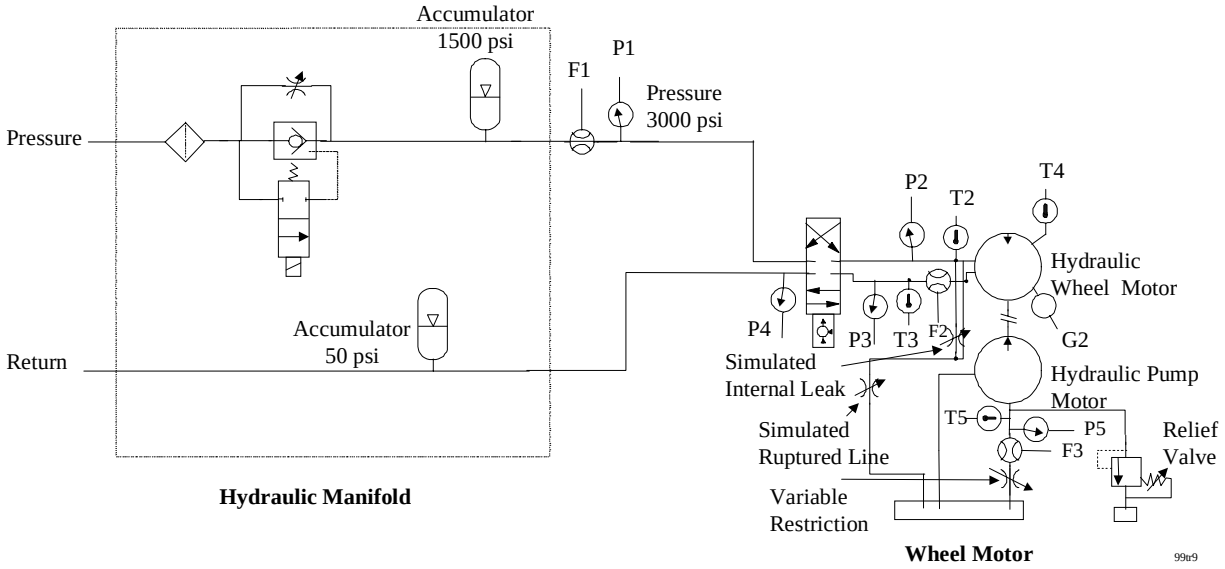

Sensor Measurement Ranges			
P1 – P3	0 to 3000 psi to 100 Hz	F1 – F3	0 to 10 gpm turbine flow meter
P4	0 to 100 psi to 100 Hz	I1 – I3	0 to 50 A, 3-phase ac current*
P5	0 to 5000 psi to 100 Hz	L1	0 to 2 in. liquid level*
T1 – T5	K-type thermocouples (60°F to 200°F)*	K1	ac power, 0 to 50 kW (not shown)
G1 – G2	0 to 1 g acceleration (100 Hz)*		

*Sensors T1, G1, I1 - I3, and L1 are not shown on the test rig diagram as these sensors were included on the HPSS.

Figure 2. Test Rig Hydraulic Schematic

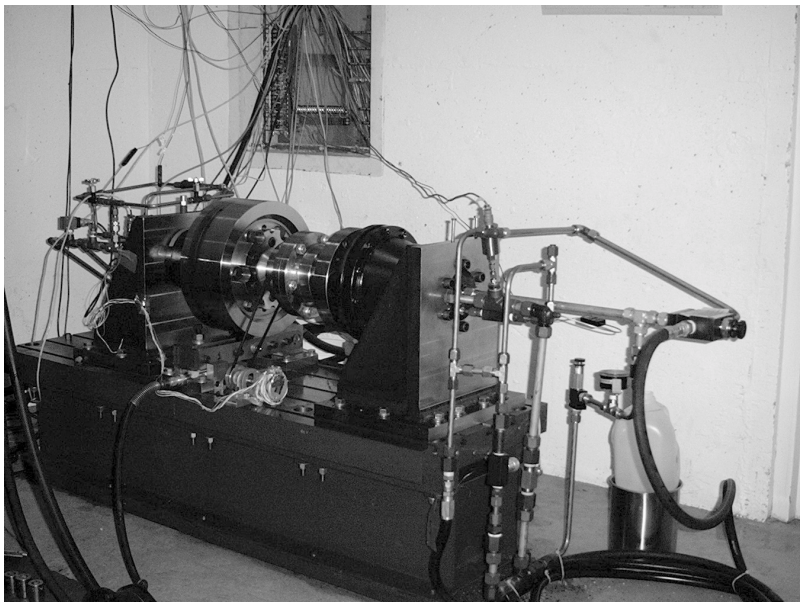

Figure 3. Test Rig Assembly

Sensors to measure pressure, flow, temperature, vibration, speed, and liquid level were placed at key locations on the hydraulic power supply and the wheel motor test rig to provide raw data for diagnostic assessments. Additional sensors and gauges were placed in the loading circuits to determine the actual loads imposed during testing.

Overall control of the test rig was provided by a combination of manual and computer control. A manual hydraulic jack and a pressure gauge were used to adjust the dead load on the wheel motor. A calibrated orifice valve was used to vary the backpressure on the loading pump and set the dynamic load on the wheel motor.

In Rosie, wheel motor control is implemented by an operator joystick that sets the control input, which is then processed by an analog proportional-integral-derivative (PID) velocity control loop. For the test rig, a custom LabView control program was used for high-level control and allowed the test operator to set the speed (0 to 20 rpm), control profile, and (PID) loop parameters of the wheel motor. The PID controller was configured to provide a control algorithm similar to the loop used in Rosie. Wheel velocity feedback was provided by an encoder mounted on the wheel motor. The loop control output was updated at a rate of 50 Hz.

The control output was supplied to an analog servovalve drive amplifier that, in turn, drove the servovalve. The servovalve amplifier handled low-level servo control functions such as antistick dithering and matched the drive power requirements of the valve.

Following assembly of the test rig, baseline data to characterize unfaulted operation of the rig were acquired at test conditions of zero speed and zero load.

2.2 Fault Selection and Simulation Methods

The failure modes for fault insertion were selected based on likelihood of occurrence, potential impact on operation of the robot, and potential for detectability, that is, the failure is not a sudden, catastrophic type that occurs with no prior warning. The challenge was to devise methods whereby each implanted fault was representative of an actual fault. The implanted fault had to be inserted and removed reliably and

repeatably. The following paragraphs outline the fault selection process and the methods devised for fault simulation.

Faults were selected from the results of an extensive Failure Modes and Effects Analysis (FMEA) and fault tree analysis of the Rosie Worksystem prepared under DOE contract DE-AR21-95MC32093 and documented in MTI 97TR19 (Jammu, 1997). Individual components in the HPSS and wheel motor were identified and the possible failure modes compiled. Each failure mode was assigned a criticality, probability, and speed of failure value. Fault tree analysis for both subsystems were performed to identify the origin and propagation of failures in the robot components. During this process, three criticality categories were assigned to each component:

- Category I: possible damage to robot or work area; self-removal may not be possible
- Category II: work assignment cannot be completed; self-removal may be possible
- Category III: work assignment can be completed; maintenance is necessary.

For the HPSS, Category I faults involved the relief valve (leaking, sticking, damaged seat); the hydraulic pump (seal failure, piston/rotor/vane damage); the pump drive motor (bad commutator brushes if dc power, open winding or rotor bars if ac induction); and the cooler (leakage, air-side plugging, fan/motor failure), as well as the usual cracked hoses or leaking connections. Category II faults affected mainly the cooling fan/motor that would lead to fluid overheating and restrict operating time, and Category III faults involved mainly filter problems and relief valve damage.

For the wheel motor, all faults were listed as Category II, based on the assumption that only one wheel motor fails and that either the shaft does not lock up or the wheel can be dragged by the other three that are still in serviceable condition. These faults mainly involved potentiometer drive belt problems/breakage, hose cracking/leakage and loose fittings, and damage to internal components such as vanes/casing/pistons. Bearing and gear faults also were noted, but were judged to be low in probability of occurrence. Finally, flow control valves were common to virtually all systems. These valves can experience faults ranging from Category 1 through 3, and often involve spool sticking, seal leakage, or electrical faults.

Based on these considerations, a list of 13 faults was developed, as shown on Table 1 and explained in the following paragraphs. Faults 1 through 7 were related to the HPSS, and Faults 8 through 13 to the wheel motor. For each fault, the method of fault insertion was chosen to simulate an actual fault as accurately as possible. For faults that generally occur suddenly, computer-controlled relays were used to insert the fault during a test sequence when feasible. This method allowed simulation of transient behavior associated with the fault occurrence as well as the end effect of the fault.

HPSS Faults

1. ***Plugged High-Pressure Filter.*** This fault was simulated by inserting a restriction in the pressure feed line to the test rig. Based on data from the filter manufacturer, the restriction was set to cause a 50-psi pressure drop at full load of the HPSS. This fault was inserted and removed during the test sequence. Reduced load capacity of the HPSS at high load levels of the wheel motor and a rise in oil temperature were the expected results.

2. ***Loss of Accumulator Charge.*** This fault was simulated by discharge of the main pressure line accumulator and was present throughout the test sequence. Variations in line pressure during transient events were the expected result.

3. ***Pump Drive Motor Fault.*** This fault was simulated by removal of one phase fuse in the three-phase ac supply for the pump drive motor. This fault represented a large class of motor faults that cause vibration and reduce motor capacity. Reduction in HPSS capacity and increased motor vibration and temperature at high load levels of the wheel motor were the expected results.

4. ***Loss of Oil Cooling.*** The fault was simulated by turning off the supply valve for the cooling water heat exchanger. The system was run without faults until the cooling water reached its equilibrium temperature of 140°F prior to fault insertion. Higher-than-normal temperatures during operation were the expected result.

5. ***Scored Pump Housing.*** A damaged hydraulic pump was installed in the HPSS. Internal scoring on this pump prevented its operation at full capacity. Reduced capacity at high loads and increased vibration, temperature, and drive motor power were the expected results.

6. ***Pump Internal Leakage.*** Upon analysis, this fault was found to duplicate the fault manifestation of Fault 5. Therefore, this fault was not inserted.

7. ***Broken Relief Valve Spring.*** The relief valve in the HPSS regulates the output pressure to a preset value. A broken or weak spring will reduce the pressure from its preset value. This fault was inserted by backing out the spring adjustment screw until the pressure was 600 psi below normal pressure. Significantly reduced capacity of the HPSS at high load conditions was the expected result.

Table 1. Implanted Faults

Fault No. and Component	Fault	Method of Detection	Method of Installation
HPSS			
1. High-pressure filter	Plugged	Low-load side pressure and flow at high-load conditions and rise in oil temperature	Variable restriction in feed pressure line
2. Accumulator	Loss of charge	Poor transient response	Discharge accumulator
3. Pump drive motor (ac)	Motor fault; open winding	Case vibration and motor current	Remove fuse from one ac phase
4. Cooling fan	Loss of oil cooling; open winding (Rosie fault)	Pump motor and fluid temperature increases	Shut off cooling water flow
5. Hydraulic pump	Scored housing	Low output pressure/flow, vibration	Use existing damaged pump
6. Hydraulic pump	Internal leakage	Increased flow to tank	Remove internal seal or install broken seal
7. Relief valve	Broken spring	Low pressure	Install weak or broken spring
Wheel Motor			
8. Hydraulic motor	Loss of casing oil	Vibration	Bleed casing oil
9. Control valve	Open winding	Change in delta P or flow	Relay-controlled line break
10. Control valve	Sticking valve	Change in delta P or flow	Change control profile in software
11 Hydraulic motor	Ruptured supply line	Tank level change	Tee flow to separate tank
12. Resolver	Broken belt or damaged resolver	Loss of speed control	Relay-controlled line break
13. Hydraulic motor	Internal leak	Changes in flow or pressure	Valve between feed line and return line

Wheel Motor Faults

8. ***Loss of Casing Oil.*** Loss of casing oil is the most common failure of the wheel motor and can occur due to rupture of a line in the casing circuit or failure of the casing check valve. This failure can cause rapid piston wear, motor heating, and an increase in vibration as the pistons ride on the cam without lubrication. This fault was inserted by bleeding the casing oil from the wheel motor prior to the start of the test sequence. Of the 13 faults identified, this fault was considered an advanced fault because of its potential for serious damage to the wheel motor. For this reason, we determined that Fault 8 would be the final fault run.

9. ***Open Control Valve Winding.*** This fault simulated a class of faults in which the hydraulic control valve of the wheel motor does not respond to electrical control inputs and then assumes a fixed output not dependent on the command input. A computer-controlled relay was used to simulate this fault by interrupting the command signal to the valve. Inability to operate the wheel motor was the expected result.

10. ***Sticking Control Valve.*** This fault simulates a common failure in electrohydraulic valves referred to as stick slip. Due to increased friction or particle contamination, the valve will alternately follow the input command or stick at the current position until the force trying to move the valve exceeds the frictional force holding the valve. This results in jerky operation during periods of acceleration/deceleration of the controlled device. The wheel motor control profile in the PID control software was modified to simulate this fault. The unfaulted command profile was a 10-sec ramp function, and the faulted response profile was a staircase comprised of ten 1-sec stick/slip intervals. Pressure and flow fluctuations and motor vibration were the expected results.

11. ***Ruptured Hydraulic Supply Line.*** Rupture of a supply line is a common failure in hydraulic systems. Although this may seem a trivial fault to detect, the enclosed nature of the Rosie hydraulic system and the fact that the robot is stationary for much of its operating time may hide the visible effects of this fault until fluid loss is sufficient to prevent removal of the robot. To simulate this fault, a valve was used to divert part of the main line flow from the feed pressure line to a separate reservoir. Reduced capacity of the HPSS at high loads and reduced fluid level in the main tank were the expected results of this fault.

12. ***Loss of Resolver Feedback.*** In Rosie, an encoder on each wheel motor provides speed feedback to the motor control PID loop to implement velocity control. A broken drive belt or wire can cause loss of the resolver signal. This fault was simulated using a computer-controlled relay to interrupt the speed feedback signal to the PID controller. Pressure, flow, and speed variations in the wheel motor response were the expected results.

13. ***Internal Leak in Drive Motor.*** Wear in hydraulic motors generally increases internal leakage, reducing power available at any speed in proportion to the amount of leakage. Internal leaks are caused by contaminated hydraulic fluid or operation at high temperatures, which can lead to seal deterioration. To simulate this fault, a manually controlled valve was inserted between the wheel motor feed pressure lines and the return line but after the wheel motor flow measurement sensor. The measured wheel motor hydraulic power input will then be greater than the work performed in relation to the size of the internal leak. Loss of wheel motor hydraulic efficiency was the expected result.

2.3 Instrumentation and Data Acquisition

Manifestations of the implanted faults were analyzed to determine the type and location of instrumentation needed to detect them. Table 2 lists the sensors selected for fault detection, with their location and measurement ranges shown on Figure 2. The measurement ranges were estimated from an analysis of the HPSS and characteristics of the wheel motor for a typical operating point.

The sensors were connected through appropriate signal conditioners to a central data acquisition system. The data acquisition system collected sensor data and was used by the test operator to control configuration of the test rig (see Figures 4 and 5). A Pentium 120 IBM-compatible PC with Windows 95 and LabView 5.0 served as the central computer and was equipped with a National Instruments 64-channel, 12-bit, high-speed data acquisition card. Data were acquired from all sensors at 200 Hz.

Software for control of test rig and data acquisition operations was written using LabView 5.0. A custom virtual instrument (VI) was written to control data acquisition, insert computer-controlled faults, and plot and record the data. The VI also provided run identification information (such as fault ID, test rig configuration, test conditions) in the output data files. Data were acquired at 200 Hz and saved in space-delimited ASCII format.

Figure 6 shows the operator interface of the system control VI. In the "Run Information" block, the operator could specify fault and test rig configuration information for the test data files as well as control information for data acquisition, such as scan rate. The "System Control" block allowed the test operator to set wheel motor speed and insert those faults set up for computer control. This block also provided indicators for critical test rig alarms, such as HPSS oil temperature. Shown at the right of the control VI, ten multivariable graphs allowed the operator to view all 24 channels of sensor data in real time during test operation.

Table 2. Fault-to-Sensor Mapping

Implanted Fault	Sensor Types
Plugged high-pressure filter	Pressure, flow
Loss of accumulator charge	Dynamic pressure
Pump drive motor fault	Vibration, current
Loss of oil cooling	Temperature
Scored pump housing	Pressure, flow
Pump internal leakage	Flow
Broken relief valve spring	Pressure
Loss of casing oil	Vibration, temperature
Open control valve winding	Pressure, flow
Sticking control valve	Pressure, flow
Ruptured hydraulic supply line	Fluid level
Loss of resolver feedback	Speed, flow, pressure
Internal leak in drive motor	Pressure, flow

99tr9

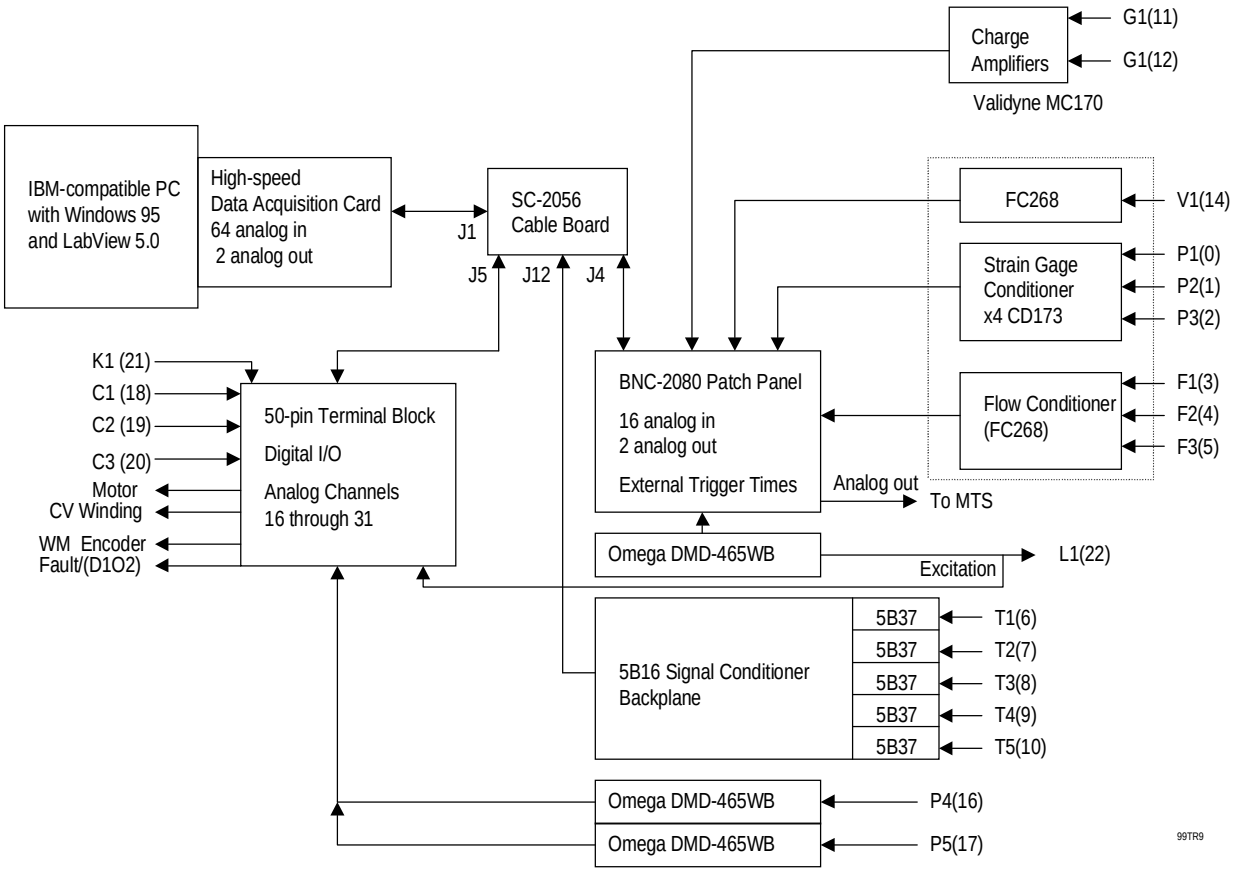

Figure 4. Test Rig Control and Data Acquisition System

Figure 5. Data Acquisition System and Control Station

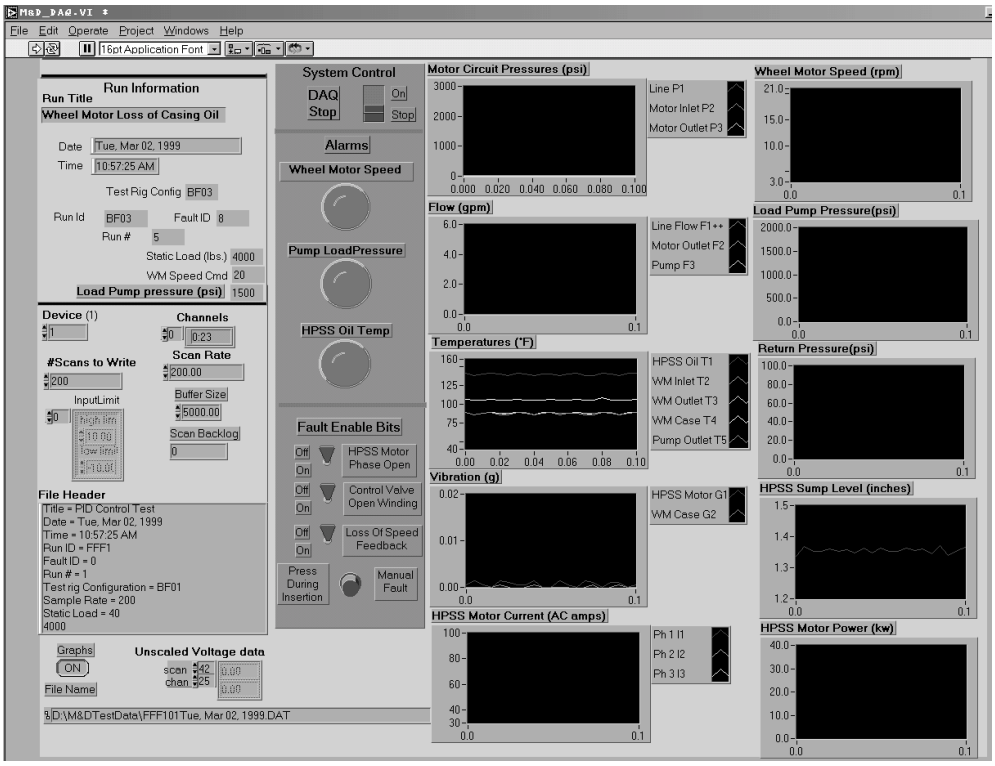

Figure 6. Data Acquisition Control Panel

2.4 Fault Insertion Procedure

The following general procedure was defined for fault insertion:

1. Start the data acquisition system and software.
2. Set all computer-controlled fault actuators to off.
3. Start the wheel motor PID control software.
4. Set the wheel motor speed command to 0 rpm.
5. Start the HPSS and allow the oil to reach normal operating temperature of 125°F.
6. Start the test rig, and set the load pressure as required for the fault and run ID. Each fault will be assessed at two speeds and two load settings.
7. If the fault is of the manual type and will be static throughout the run, insert the fault now.
8. Enter the fault and test rig information into the spaces provided on the control panel. Enter the data acquisition parameters. For most faults, set sampling rate at 200 Hz.
9. Start the data acquisition process.
10. Set the wheel motor speed to the required value for the run being performed.
11. If the fault is to be inserted under computer control, allow data acquisition to occur for 10 sec prior to insertion of the fault. Insert computer-controlled fault after this time.
12. Collect data for at least 20 sec with the fault present and then remove the fault.
13. Collect data for an additional 10 sec after removing the fault.
14. Stop data acquisition.
15. Set the wheel motor speed command to 0 rpm.

2.5 Analytical Techniques

Several types of analytical techniques were applied to the test data: analytical redundancy (AR) and derived variables, statistical, and spectral analysis.

2.5.1 Analytical Redundancy

AR is a model-based state-space technique that derives the maximum number of independent tests of the consistency of sensor data with the linearized system model and past sensor and control inputs. It yields tests to determine whether the system is performing nominally, or is deviating from the desired plan and presumably under fault conditions. AR exploits the null space of an appropriate observability matrix to derive a null space spanning set of comparisons between model and system behaviors, as seen by the sensors (Chow and Willsky, 1984; Leuschen, et al., January 1999; and Leuschen, et al., April 1999). If the physical system deviates from the model, these comparisons will not match, and information about the error can be determined from the error signal. AR is only formally defined for linear systems, but research for this project included the development of methods to extend it to nonlinear systems such as the hydraulic flow though a servovalve. Four independent linear tests were generated (V1 through V4) based on a model of the wheel motor. Tests V1 and V2 monitored linear parts of the system, and the new nonlinear techniques were applied to the V3 and V4 tests to generate the nonlinear (NV3 and NV4) tests.

Since the set of AR tests used in this study was based on a model of the wheel motor, they were not applicable to the HPSS faults because they did not model any HPSS dynamics. For the sake of completeness, the HPSS fault data were run through the AR tests anyway, but the results were uniformly negative. Separate AR analysis of the HPSS is possible, given sufficient knowledge of the system characteristics and control equations.

The AR tests applied to the wheel motor model can be interpreted as follows:

- **V1.** This test is a discretized version of the linear differential equation describing the physical dynamics of the motor and load and their relation to the pressure load across the motor. This test checks to ensure that the motor is working as expected.

  The faults investigated tended to cause large spikes in the output from this test. Since none of these faults caused large permanent changes in the characteristics of the motor, this is not surprising. The onset of the fault disturbs the entire system, momentarily causing a large fault signal. Once the disturbance settles, the undamaged motor resumes its expected behavior.

- **V2.** This test is, in some sense, the discrete time derivative of equation V1. However, it is also a blending of the hydraulic equation with the kinematic equation, so its behavior is not immediately predictable as derivative-like. AR mathematics indicates that this equation can react to faults in ways that V1 cannot.

  V2 is harder to examine than V1 since its output does not center on zero. It gives a steady-state value representing unmodeled system and load effects. Thus, the test responds to changes in system parameters by outputting a step function as these values change. As a consequence, V2 is not a good test for certain faults when the system parameters have changed for other reasons. For example, minor changes in system parameters caused by the work needed to install a simulated fault might change the steady-state value of this test.

  In the data analysis, this results in a difference bias between the V2 test result for the fault run and the one for the rig-configuration (unfaulted) run, even if the fault itself is not responsible for the bias change. This effect is misleading, but is not a cause for concern if it is understood. Small variations

in the steady-state values of this test may be safely ignored, and the test is still useful for fault detection, since sudden steps in this test represent the occurrence of a fault and are not ambiguous.

- **NV3.** This test is a discretized version of the equations representing the hydraulic characteristics of the wheel drive. NV3 examines the pressure and shaft position signals and determines if these are consistent with its model of the hydraulic system.

  NV3 responds to faults with a step function, much like test V2. This makes it as vulnerable as V2 to problems with varying system parameters. It is thus important to remember that a small steady-state difference between the fault run and rig-configuration run of this test is not necessarily significant.

- **NV4.** This test is the derivative of NV3 just as V2 is the derivative of V1 and blends the kinematic equation into the hydraulic one in similar way. In this case, the original equation exhibits the step function behavior, while the derivative, NV4, responds to faults with spikes similar to V1.

For the AR tests, it should be noted that the y-axes are arbitrary. The shape of the curve is important, its magnitude is not, as long as the scaling factor is constant between different runs of the same test. We were careful to ensure that this restriction was followed for our tests. Thus, the units and magnitudes on the AR data plots presented should be ignored. The curve shape is the focal point for the plots.

2.5.2 Derived Variables, Statistical and Spectral Analysis

In addition to the raw data, several derived parameters were calculated to investigate more performance-oriented variables (compared to flows, temperature, and pressures) that might produce good sensitivities with fewer sensors. Each sensor by itself does not give a clear picture of faulted conditions as the readings can be affected by many normal operational parameters (such as climbing) as well as by the presence of faults. Derived performance parameters, especially ratiometric ones, in many cases show less sensitivity to operational conditions and are more closely related to faulty conditions. For example, the hydraulic efficiency of a motor such as the wheel motor is relatively constant over a wide range of operational conditions but decreases for many fault conditions.

The derived parameters used in the additional analysis were:

1. Wheel motor hydraulic efficiency = load power/wheel motor power
2. HPSS efficiency = output hydraulic power/input electrical power
3. Leak detector = line pressure/line flow ^2
4. Wheel motor hydraulic power = delta P * flow/1714.

The additional analysis performed on the raw and derived data consisted of statistical and spectral processing. Statistical processing consisted of root-mean-square (rms) value, standard deviation, skewness, kurtosis, peak to peak, and crest factor. Statistics were computed for the entire data file and for 0.25-sec intervals within the data to determine statistical trends. Spectral processing consisted of a windowed fast Fourier transform on a detrended version of the data in the frequency range from 0.1 to100 Hz. Based upon the particular fault and when it was inserted and removed, spectra were generated for subregions of the data to detect changes in frequency content. Of particular interest were the amplitudes of peaks related to the wheel motor running speed and piston frequency (24x running speed).

2.6 Test Results

Test results for the wheel motor and HPSS faults are presented in the following subsections. The faults for the wheel motor are presented first, since this was the model to which the AR technique was applied. A wealth of data were generated during the test runs, and the plots presented here are typical of the results obtained during testing.

2.6.1 Wheel Motor Fault Testing

For Faults 9, 10, 12, and 13, example plots for a typical data run are presented. On each plot, a solid red line indicates a test run with the fault installed, and a dotted aqua-blue line indicates a fault-free rig configuration run (used for comparison purposes). A dashed circle highlights areas of interest in the data on each plot. The following nomenclature for test run identification was used to distinguish between runs:

- RC: defines rig characterization (no faults)
- BF: basic fault.

For the RC tests, each test was identified by run number and *fault number*, e.g., RC03*03*, designated test run 3 for fault 3. For the BF tests, a number indicating the **sequence** of the test run was added to the run and fault numbers, e.g., BF019**3**. The sequential test runs usually, but not always, followed a pattern for speed and load:

- Test sequence 1: 5 rpm, 0 psi
- Test sequence 2: 5 rpm, 500 psi
- Test sequence 3: 5 rpm, 1500 psi
- Test sequence 4: 20 rpm, 500 psi
- Test sequence 5: 20 rpm, 1500 psi.

All raw data plots were downsampled by a factor of 19 due to computer memory constraints. Down sampling of 20 gave irregular results, since there was a harmonic effect at this frequency for some data values.

Since AR tests were performed every 0.1 sec, they were effectively downsampled by a factor of 20. Unless noted otherwise, all x-axes are time in seconds, and the y-axes are arbitrary. The shape of the curve, not its magnitude, is important, since the scaling factor was kept constant between the different tests.

As indicated in Section 2.2, Fault 8 was considered an advanced fault due to the potential for serious damage to the wheel motor. Results of testing for this fault are discussed in Section 2.6.3.

2.6.1.1 Fault 9: Open Control Valve Winding

As shown in Figure 7, the onset and duration of this fault is clear in all AR tests. The open winding acts like a step input that was not accounted for in the model, which provokes a strong AR response.

2.6.1.2 Fault 10: Sticking Control Valve

This fault was evident on all AR tests, although V1 and NV4 showed the clearest results (see Figure 8). During the portions of the run where the system was stuck, it did not follow the dynamic model at all, and was thus easy to detect.

2.6.1.3 Fault 11: Ruptured Hydraulic Supply Line

AR did not detect this fault, even for relatively large leaks, unless the system was idling. We believe this occurred because raw flow measurements can detect large leaks but are not sensitive to small ones. However, small leaks could be detected by combining flow monitoring with a sump-level sensor. Flow could be monitored by either comparing flow through the motor with theoretically predicted flow or by measuring flow consistency between different sensors. Although our sump monitoring showed no significant decrease for these tests, a sump-level sensor is still a good idea.

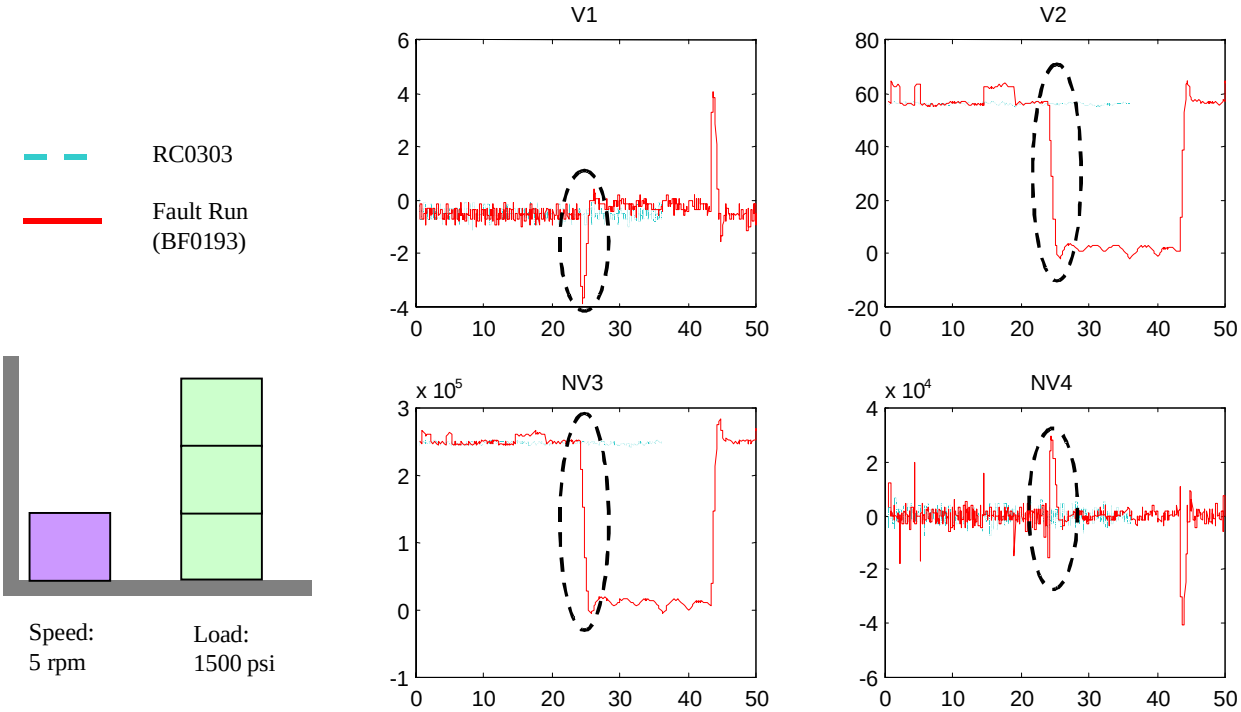

Figure 7. Fault 9: Open Control Valve Winding

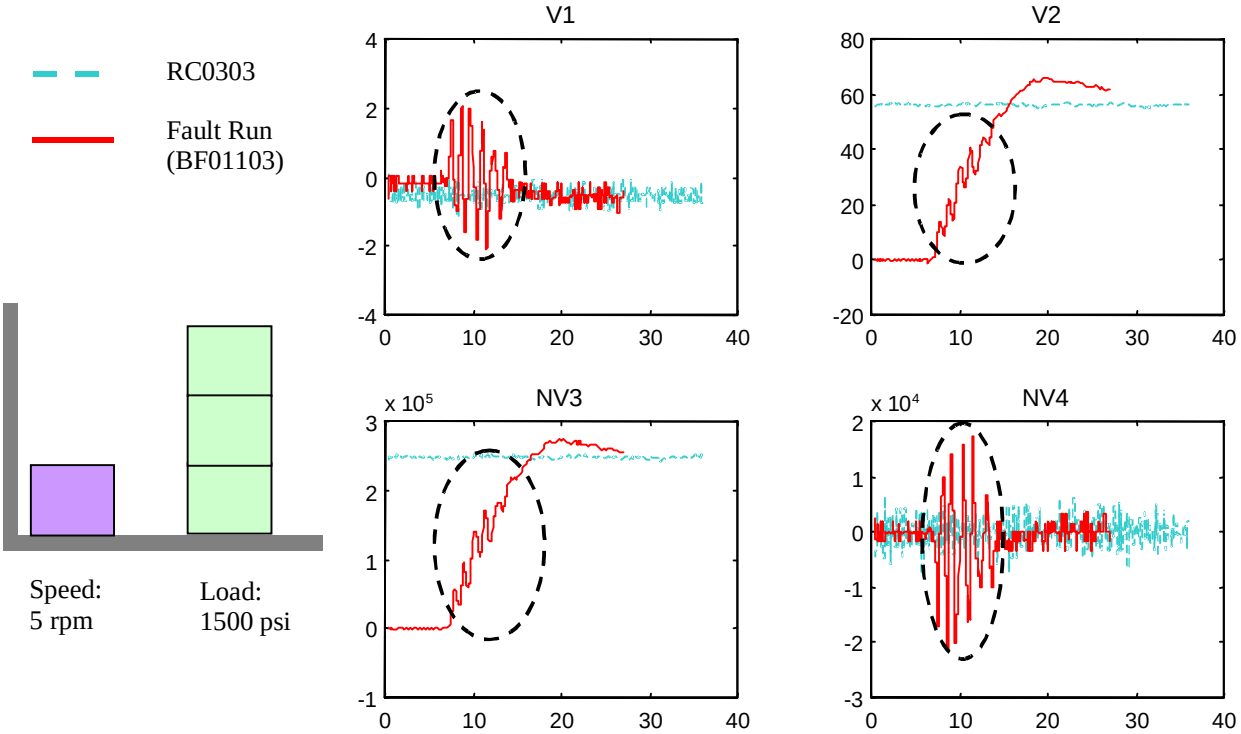

Figure 8. Fault 10: Sticking Control Valve

Work performed on a robotic spray system has shown that the calculated parameter, pressure divided by flow squared, is an excellent means of detecting a catastrophic leak in a high-pressure line (Foster-Miller, KARL1B Robotic Spray System, U.S. Navy contract). During field operation of this high-pressure robotic spray system, this parameter was monitored, and the high-pressure pump tripped when the value deviated by more than 30% from the expected value, thereby preventing continued fluid loss.

2.6.1.4 Fault 12: Loss of Resolver Feedback

Except for the idling system, AR performed well in detecting this fault (see Figure 9). The idling system was already giving a near-zero value for the zeroed-out sensor. If idling, it would alert the user as soon as the wheel motor speed was increased. Since the failed sensor invalidated the control loop, AR detected this as a deviation from the model-expected behavior.

2.6.1.5 Fault 13: Internal Leak in Drive Motor

The best test for this fault was to let the system idle and then compare the pressure drop across the motor ports. When there was a low load, the effects of the leak were most prominent as shown on Figure 10. The measurement of the pressure drop across the motor ports was needed for the AR test (or any other model-based error detection scheme). Small internal motor leaks will continue to remain difficult to detect during periods of heavy use.

2.6.2 HPSS Fault Testing

As stated earlier, the AR tests used in this research were based on a model of the wheel drive and were thus not widely applicable to the HPSS faults, since they did not model any HPSS dynamics. For the sake of completeness, the HPSS fault data were run through the AR test, but the results were uniformly negative. Since the HPSS was not included in the AR model, conventional statistical and spectral analyses were performed in an attempt to reveal variables that could be included in an AR model of the HPSS. The derived parameter of HPSS efficiency, H_{eff}, was of particular interest. Machine efficiency has been shown in other contexts (gas turbine engines, for example) to be a more robust indicator of faults than individual parameters alone.

2.6.2.1 Fault 1: Plugged High-Pressure Filter

For the plugged filter fault, we expected that the HPSS drive motor would have to work harder to produce a given amount of output power. Figure 11a shows the rms value calculated for hydraulic efficiency taken at 0.25-sec intervals during the rig characterization run (RC0405), and Figure 11b shows the same plot for the faulted run (BF0115) with the plugged filter. As shown, the efficiency dropped from 0.13 to 0.11 in the presence of the plugged filter.

This fault was most prominent when there was a heavy load on the system. Even then, it would be hard to detect using AR tests and depends on a steady, predictable HPSS pressure. Further, several independent systems draw pressure from the HPSS in the Rosie system, rather than the single system examined here.

2.6.2.2 Fault 2: Loss of Accumulator Charge

Faulty runs were conducted with the HPSS accumulator deliberately discharged. Although, in theory, this should have caused problems with the source pressure, our results showed little change in the overall behavior of the system. Since the accumulator is essentially a low-pass pressure filter, this fault could most likely be detected by frequency domain tests of the HPSS output pressure data.

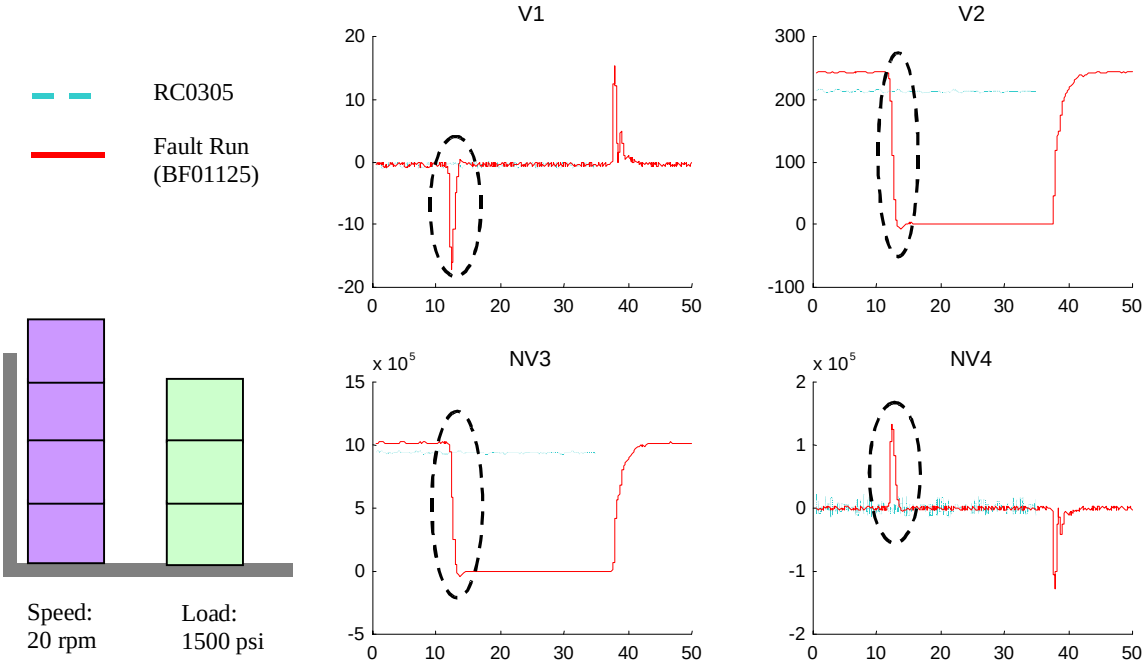

Figure 9. Fault 12: Loss of Resolver Feedback

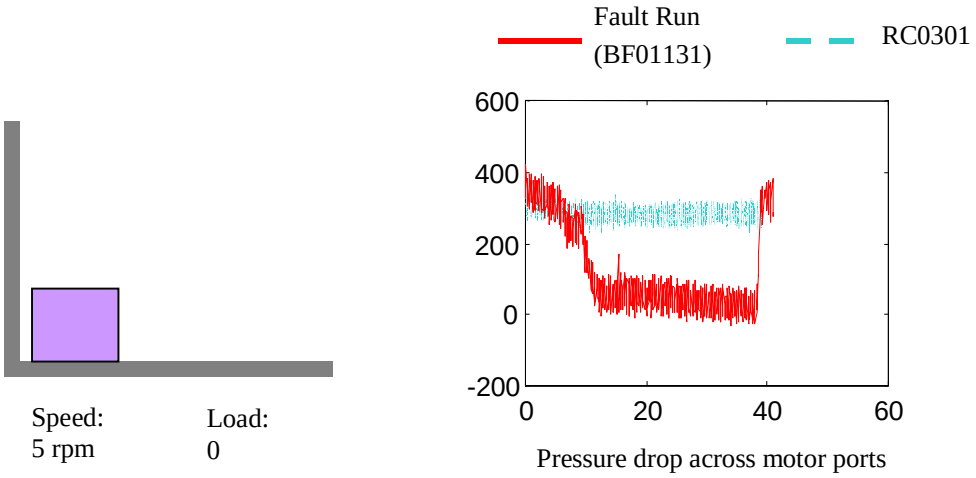

Figure 10. Fault 13: Internal Leak in Drive Motor

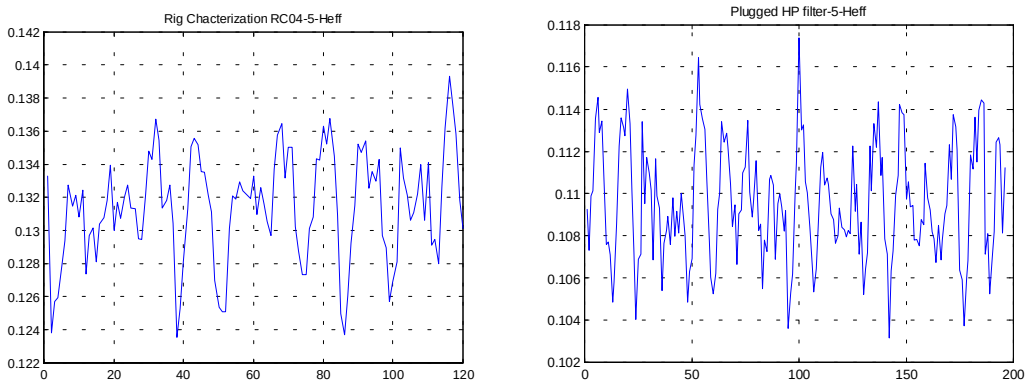

a. Baseline ***b. Plugged High-Pressure (HP) Filter***

Figure 11. Fault 1: Hydraulic Efficiency Change

Comparison of the spectra of the feed pressure and flow between the faulted and unfaulted case did not reveal any differences in the spectral peaks related to the piston frequency at 20 rpm (8 Hz). In the unfaulted run, a much larger peak was noted at the running frequency of 0.33 Hz. The cause of this peak is unknown.

2.6.2.3 Fault 3: Pump Drive Motor Fault

Figure 12 presents the results of testing for Fault 3. RC data are not shown since all three currents would show constant value for the rig configuration run and power consumption (kW) would also remain constant. As the figure indicates, the HPSS power consumption and winding currents provided very clear indications of the open winding fault. If either of these parameters is monitored, this fault should be easy to detect by comparing the HPSS output to these signals

The pressure output of the HPSS was deliberately lowered for this test to prevent the pump from overloading the breaker. Since this precaution is unlikely in a working system, monitoring of the pressure output may be another useful technique.

Comparison of the rms value of the hydraulic efficiency for the unfaulted (0.11) and faulted (0.086) cases showed that the hydraulic efficiency decreased as expected.

2.6.2.4 Fault 4: Loss of Oil Cooling

This fault demonstrated the application of hydraulic efficiency to detect HPSS anomalies. Figure 13a shows the temperature increase during the faulted run, and Figure 13b shows the rms value of the hydraulic efficiency. The subtle upward trend in efficiency (probably due to decreased viscosity in the hotter oil) is clearly visible above the much larger noise level on Figure 13b.

As an alternative to using hydraulic efficiency to detect this fault, it would also be possible to monitor the slope of the temperature curve, compare it to an AR-style test that compensated for the system load, and issue an earlier warning. This approach would require greater knowledge of the system's thermodynamic characteristics, but would allow for quicker detection of cooling system failure.

2.6.2.5 Fault 5: Scored Pump Housing

As expected, AR tests for this fault were inconclusive, although, in theory, AR tests based on an HPSS model might detect this fault. Figures 14a and 14b show the results. As shown in Figure 14b, a change in hydraulic efficiency was noted in the direction expected. The scored housing fault results in lower hydraulic efficiency for the pump due to increased internal leakage. This, in turn, results in lower overall efficiency.

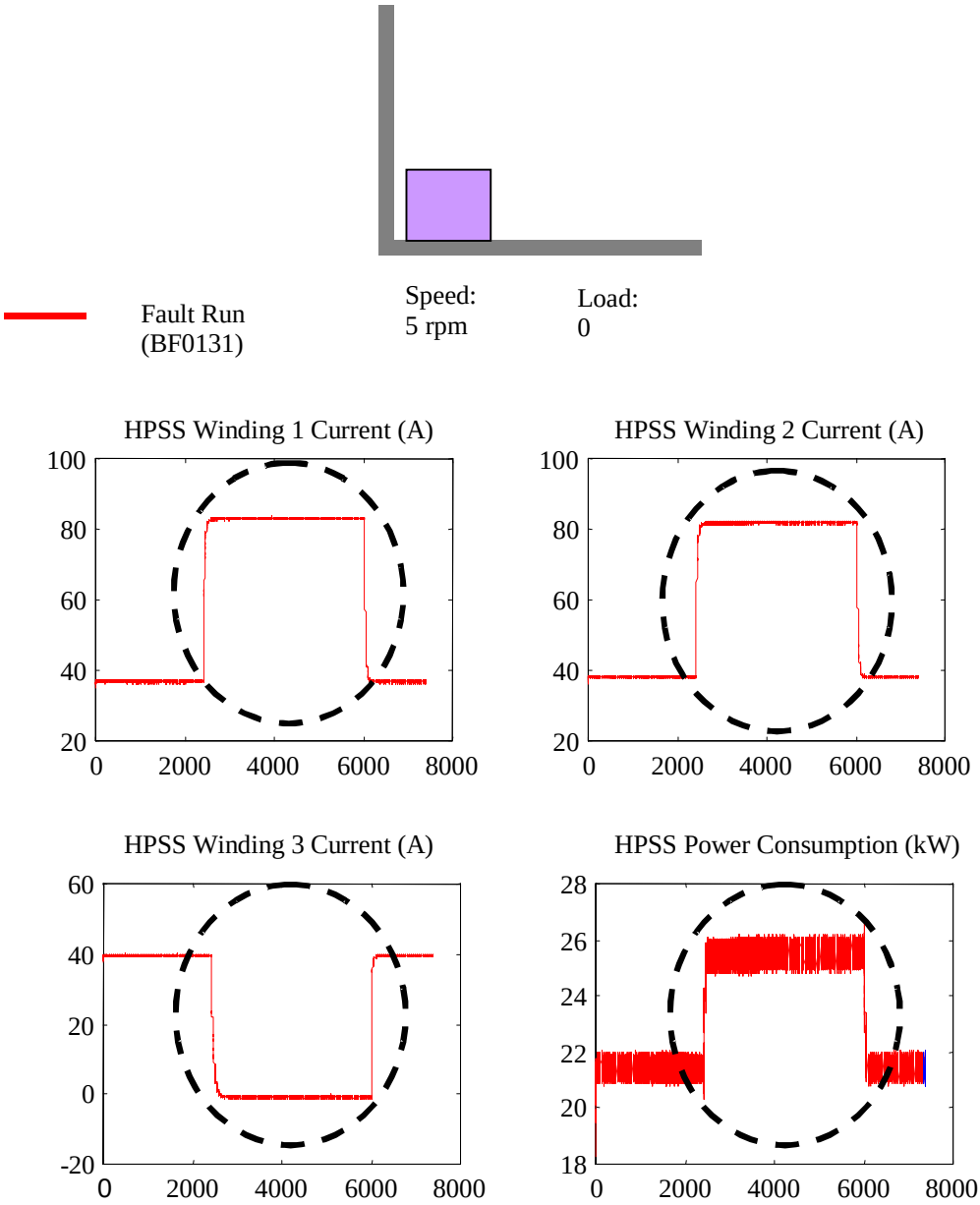

Figure 12. Fault 3: Pump Drive Motor Fault. Winding currents and power consumption at 5 rpm and 0 psi for fault run. (Time scales multiplied by 200).

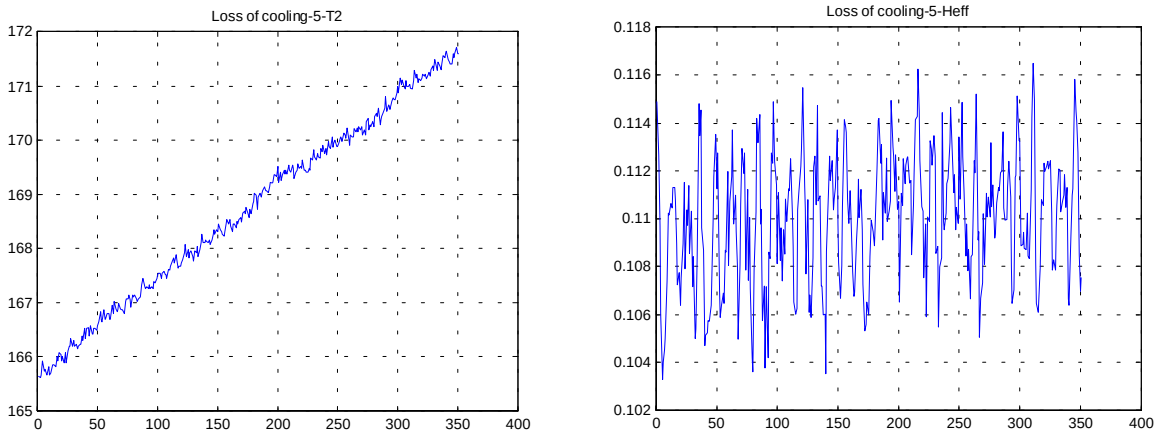

a. Hydraulic Fluid Temperature ***b. Hydraulic Efficiency (rms value)***

Figure 13. Fault 4: Loss of Cooling Oil

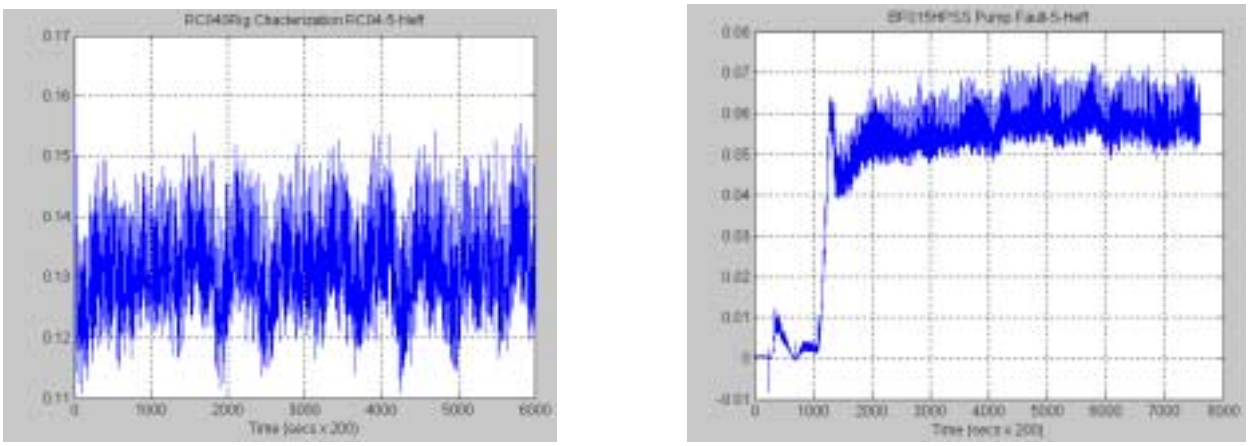

a. Unfaulted RC Test ***b. Change due to Implanted Fault***

Figure 14. Fault 5: Scored Pump Housing

2.6.2.6 Fault 7: Broken Relief Valve Spring

As shown in Figure 15, this fault was easily detected by monitoring the inlet pressure and use of an AR technique is not necessary. Further, although the pressure loss was not caused exclusively by this fault, drastic drops in pressure should alert the user to a problem in any case.

This fault did cause an apparent decrease in hydraulic efficiency, but the drop was probably attributable to the lower output pressure and not a loss in efficiency. The fault does provide a good demonstration of the fact that hydraulic efficiency cannot be considered alone but must be used in a model-based system that predicts it under various operating conditions.

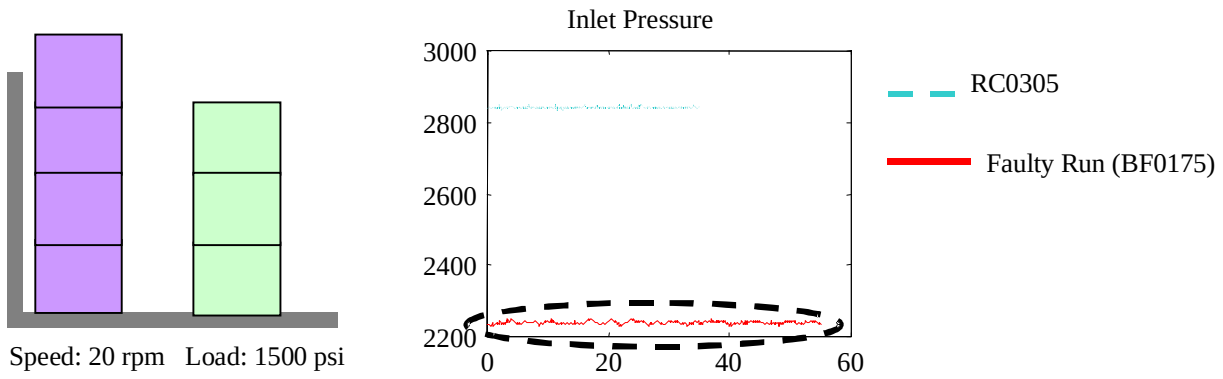

Figure 15. Fault 7: Broken Relief Valve Spring

2.6.3 Advanced Fault Testing

Fault 8, loss of casing oil, was considered an advanced fault because of the potential for serious damage to the wheel motor and was therefore the final fault test run. However, we were unsuccessful in our attempts to implant this fault. It is important to note that the wheel motor design is such that the casing will not fill with oil via normal internal leakage. To prepare for eventual implantation of Fault 8, the motor casing was filled with oil through a bleed port during the initial start-up of the test rig. To implant the fault, we later drained the oil from the casing through the bleed port and conducted a test run. However, after the test run, it was discovered that the casing was again full of oil. The test was repeated twice to determine if the effect was constant, and the casing remained full. We attributed the effect to an internal leak that developed at some time during the test program, which could have resulted from normal wear in the motor or an internal motor fault. For this reason, we could not implant Fault 8 and operate the test rig at speed and load without casing oil.

During the course of attempting to implant Fault 8, the static load was improperly set at twice the intended value. Since operation of the test rig without casing oil was unsuccessful, the data resulting from this overload was reviewed in the context of a new advanced fault, bearing overload. The bearing overload fault was not made obvious by application of either the AR method or unprocessed data analysis.

2.7 Conclusions and Recommendations

The AR technique was shown to be effective in detecting faults in the wheel motor. Extension of this model for the wheel motor to include the HPSS will be required before AR diagnostics can address the full list of faults necessary for a complete robot system such as Rosie.

Performance-based assessment variables may provide an efficient means of detection while simultaneously minimizing the number of sensors required. This approach may increase the reliability of the diagnostic system. However, in any diagnostic system, additional diagnostic information gained from additional sensors must be traded off against the decrease in overall reliability of the diagnostic system due to its increased complexity.

Even though derived parameters, such as HPSS efficiency, demonstrated sensitivity to detect even subtle faults (such as oil viscosity change due to overtemperature), such detection was made under equivalent conditions. A model of the HPSS efficiency would be required to provide robust detection under the widest variety of operating conditions.

Many traditional diagnostic assessment techniques, such as spectral, envelope, and statistical analyses, require steady-state operation of the monitored machine in order to provide useful results. The typical operating regime of a robot such as Rosie includes operations that are either highly variable or transient in nature. Model-based approaches that incorporate input from multiple sources to evaluate normal and abnormal performance are necessary for these types of robots. Augmentation of AR diagnostics with traditional vibration analysis for steady-state elements such as the HPSS electric motor will provide complete coverage for all anticipated faults.

New techniques, such as joint time frequency analysis and wavelet analysis, are being applied to nonstationary processes with good results. This research project produced a large amount of data that could be analyzed in future work using improved AR models and time-frequency techniques.

3.0 RELEVANCE, IMPACT, AND TECHNOLOGY TRANSFER

3.1 Research Focus on Critical DOE Problems

The results of this project demonstrate that AR fault detection is an appropriate monitoring method for hydraulic robot systems such as Rosie and other DOE systems that must operate in hazardous environments. Safety and reliability are critical to the success of cleanup operations. To the best of our knowledge, the work performed in this research project represents the first detailed examination or fault detection for these types of hydraulic robot systems.

3.2 Research Contribution to Improved Technologies and Cleanup Approaches

Better fault detection for hydraulic robot systems will reduce the costs associated with their failure in the workplace by minimizing the damage done by and to faulty systems. Application of the fault detection methods developed as a result of this research will increase confidence in the safety of hydraulic robot systems and thus lead to their increased use. The timeliness and effectiveness of DOE cleanup operations will benefit from the increased use of robot systems.

3.3 Research Contribution to Bridge Gap between Fundamental Research and Applied Technology

Previous theory for rigorous model-based fault detection such as AR has been limited to linear systems, which is not appropriate for hydraulically driven robots. The nonlinear AR methods developed in this research project are of considerable theoretical interest as well as directly applicable to fault-detection methods for any significantly nonlinear system. The wheel drive examined in this research is a particularly good example of a nonlinear system in heavy use today.

3.4 Project Impact

This project is the first evaluation of model-based diagnostics to hydraulic robot systems. The effectiveness of the model-based diagnostic technique was demonstrated and expansion to full-scale field application is warranted. Development of nonlinear AR techniques continues at Rice University through the work of Dr. Walker at Clemson University, Dr. Cavallaro at Rice University, and Martin Leuschen, a Ph.D. candidate at Rice University and a key contributor to this research project.

3.5 Justification for Larger-Scale Trials

The ability to provide meaningful diagnostics for hydraulically driven robots has been verified as a result of this research and a greater understanding of how to detect faults in hydraulic systems has been gained.

Further, this work has demonstrated the applicability of model-based fault detection to hydraulically driven robots. The AR model for the wheel drive has been developed and shown to be effective in identifying faults that could prevent successful completion of cleanup tasks by hydraulic robots.

The nonlinear AR technique is a new model, and its expansion to include additional critical components of a robot system is the next step. We recommend that a larger effort, involving a more extensive set of faults and systems, be conducted to refine the algorithms developed during this research, in order to extend our understanding and focus the results on current DOE systems.

3.6 Improved Scientific Capabilities

The investigators on this project have developed a much deeper familiarity with and understanding of the failure characteristics of the drive systems of hydraulic robots. A new mathematical fault detection technique, nonlinear AR, has been developed and applied. Further research into the technique is proceeding, and the results of this work will provide other interested scientists with valuable insight into its application.

3.7 Advances in Understanding of Technology

This project has made two advances in the understanding of the technology needed to detect faults in hydraulic robot systems. First, a greater understanding of fault detection of the class of nonlinear systems characterized by hydraulic drives has been gained, and extensive empirical data have been acquired and analyzed. Second, new theoretical nonlinear fault detection models have been generated and evaluated using these data.

3.8 Additional Scientific Hurdles

The results specific to the hydraulic test rig used in the project would benefit from more repetitions to increase statistical confidence. As noted above, we recommend funding of a follow-on project to allow the collection of significantly more data from a similar empirical test bed, and pilot studies of fault detection on actual DOE hydraulic robot systems.

3.9 Interest Expressed by Other Parties

The scientific community has expressed interest in the results of this research project as evidenced by the following papers accepted for presentation at two conferences focused on issues that impact robot systems used in DOE's EM operations.

- Leuschen, M. L., I. D. Walker, and J. R. Cavallaro. "An Investigation of Reliability of Hydraulic Robots for Hazardous environment using Analytical Redundancy." *Proceedings of IEEE Annual Reliability and Maintainability Symposium*, Washington, D.C., January 1999.
- Leuschen, M. L., I. D. Walker, and J. R. Cavallaro. "Monitoring and Diagnostics for a Hydraulic Robot in Hazardous Environments." *Proceedings of ANS 8th Topical Meeting on Robotics & Remote Systems*, Pittsburgh, PA, April 1999.
- Leuschen, M. L., I. D. Walker, J. R. Cavallaro, R. Gamache, and M. Martin. "Experimental AR Fault Detection Methods for a Hydraulic Robot." *Proceedings of the 18th International Systems Safety Conference*, Fort Worth, TX, September 2000.

4.0 PROJECT PRODUCTIVITY

The project accomplished the research objectives. A test rig capable of providing realistic loads to the wheel motor to simulate in-service robot operation was designed and built. The rig was instrumented to monitor key parameters needed to determine diagnostic approaches for fault identification. A list of faults were identified, and successfully implanted in the test rig, with the exception of the casing oil fault. Data for the majority of faults were acquired at three load settings for 5 rpm and two for 20 rpm. For certain faults, fewer or more settings were tested. Analysis of the data indicated that the AR technique was effective in identifying wheel motor faults.

The project schedule was delayed due to transition of the project from Mechanical Technology Inc. (MTI) to Foster-Miller Technologies, following the sale of MTI's Technology Division to Foster-Miller. During this transition, the rig was moved to a different facility and reinstalled to complete the test program.

5.0 PERSONNEL SUPPORTED

The personnel supported by this research included:

- Michael Martin, FMT, principal investigator
- Joseph Tecza, FMT, original principal investigator, rig design and test plan
- Jack Hamil, FMT, technician, rig fabrication and assembly
- Jason McDowell, FMT co-op student, Clarkson University, test engineering support
- Ronald Gamache, RWG Technology Solutions, development of LabView virtual instrument, design of the data acquisition and motor control systems, and test engineering support
- Martin Leuschen, Rice University, data analysis and extension of AR technique to nonlinear analysis.
- Dr. Ian Walker, Clemson University, and Dr. Joseph Cavallaro, Rice University, provided guidance for the activities of Martin Leuschen.

6.0 PUBLICATIONS

The following publications resulted from this research.

1. Leuschen, M. L., I. D. Walker, and J. R. Cavallaro. "An Investigation of Reliability of Hydraulic Robots for Hazardous environment using Analytical Redundancy." *Proceedings of IEEE Annual Reliability and Maintainability Symposium*, Washington, D.C., January 1999.
2. Leuschen, M. L., I. D. Walter, and J. R. Cavallaro. "Monitoring and Diagnostics for a Hydraulic Robot in Hazardous Environments." *Proceedings of ANS 8th Topical Meeting on Robotics & Remote Systems*, Pittsburgh, PA, April 1999.
3. Leuschen, M. L., I. D. Walker, and J. R. Cavallaro. "Data Analysis of Hydraulic Fault Data from Foster-Miller Testbed." Rice University Technical Report TR9911, Rice University, 1999.
4. Leuschen, M. L., I. D. Walker, and J. R. Cavallaro. "Fuzzy Markov Modeling for Reliability." To be published in *Reliability Engineering and System Safety*.
5. Leuschen, M. L., I. D. Walker, and J. R. Cavallaro. "Application of Nonlinear Extended Analytical Redundancy to a Hydraulic Actuator." To be submitted to *Journal of Robotic Systems*.

6. Leuschen, M. L. "Implementing and Refining Analytical Redundancy for a Nonlinear Hydraulic Robot." Ph.D. Thesis in preparation for defense in Spring of 2001.
7. Leuschen, M. L., I. D. Walker, J. R. Cavallaro, R. Gamache, and M. Martin. "Experimental AR Fault Detection Methods for a Hydraulic Robot." *Proceedings of the 18th International Systems Safety Conference*, Fort Worth, TX, September 2000.

7.0 INTERACTIONS

The research project resulted in the following participation and presentations at meetings related to robotic systems used in DOE cleanup operations.

1. Martin, M. R. Environmental Management Science Program Workshop. 1998.
2. Leuschen, M. L., I. D. Walker, and J. R. Cavallaro. "An Investigation of Reliability of Hydraulic Robots for Hazardous environment using Analytical Redundancy." *Proceedings of IEEE Annual Reliability and Maintainability Symposium*, Washington, D.C., January 1999.
3. Leuschen, M. L., I. D. Walter, and J. R. Cavallaro. "Monitoring and Diagnostics for a Hydraulic Robot in Hazardous Environments." *Proceedings of ANS 8th Topical Meeting on Robotics & Remote Systems*, Pittsburgh, PA, April 1999.
4. Leuschen, M. L., I. D. Walker, J. R. Cavallaro, R. Gamache, and M. Martin. "Experimental AR Fault Detection Methods for a Hydraulic Robot." *Proceedings of the 18th International Systems Safety Conference*, Fort Worth, TX, September 2000.

8.0 TRANSITIONS

The enabling research conducted at Rice University prior to and during this research project is continuing under Dr. Cavallaro's and Dr. Walker's supervision of the preparation of Martin Leuschen's Ph.D. thesis.

9.0 PATENTS

No new discoveries, inventions, or patent disclosures were made as a result of this research project.

10.0 FUTURE WORK

Further theoretical work into nonlinear AR is planned. Although current techniques model nonlinear systems after equivalent linear systems, future techniques will derive AR directly from the nonlinear model, using rigorous nonlinear control theory. Extension of AR models to other hydraulic components, specifically the HPSS, is needed before development of a full diagnostic package for hydraulic robots.

No future work has been identified with DOE.

REFERENCES

Chow, E. Y. and A. S. Willsky. "Analytical Redundancy and the Design of Robust Failure Detection Systems." *IEEE Transactions on Automatic Control*, AC-29(7):603-614, July 1984.

Jammu, V. "Diagnostics and Data Fusion for Robotic Sensing, Volume I: Analysis of Diagnostic/Prognostic Technologies." Final Report for DOE Contract DE-AR-21-95MC32093, MTI 98TR9, June 1997.

Leuschen, M. L., I. D. Walker, and J. R. Cavallaro. "An Investigation of Reliability of Hydraulic Robots for Hazardous environment using Analytical Redundancy." *Proceedings of IEEE Annual Reliability and Maintainability Symposium*, Washington, D.C., January 1999.

Leuschen, M. L., I. D. Walter, and J. R. Cavallaro. "Monitoring and Diagnostics for a Hydraulic Robot in Hazardous Environments." *Proceedings of ANS 8th Topical Meeting on Robotics & Remote Systems*, Pittsburgh, PA, April 1999.

Leuschen, M. L., I. D. Walker, J. R. Cavallaro, R. Gamache, and M. Martin. "Experimental AR Fault Detection Methods for a Hydraulic Robot." *Proceedings of the 18th International Systems Safety Conference*, Fort Worth, TX, September 2000.